

# Author's Accepted Manuscript

Longitudinal measurements of postnatal rat brain mechanical properties in-vivo

Alice C. Pong, Lauriane Jugé, Shaokoon Cheng, Lynne E. Bilston



PII: S0021-9290(16)30437-7  
DOI: <http://dx.doi.org/10.1016/j.jbiomech.2016.04.005>  
Reference: BM7683

To appear in: *Journal of Biomechanics*

Received date: 10 December 2015  
Revised date: 8 February 2016  
Accepted date: 4 April 2016

Cite this article as: Alice C. Pong, Lauriane Jugé, Shaokoon Cheng and Lynne E Bilston, Longitudinal measurements of postnatal rat brain mechanical properties in - v i v o , *Journal of Biomechanics*  
<http://dx.doi.org/10.1016/j.jbiomech.2016.04.005>

This is a PDF file of an unedited manuscript that has been accepted for publication. As a service to our customers we are providing this early version of the manuscript. The manuscript will undergo copyediting, typesetting, and review of the resulting galley proof before it is published in its final citable form. Please note that during the production process errors may be discovered which could affect the content, and all legal disclaimers that apply to the journal pertain.

Longitudinal measurements of postnatal rat brain mechanical  
properties in-vivo.

Alice C. Pong<sup>1 †</sup>, Lauriane Jugé<sup>1,2 †</sup>, Shaokoon Cheng<sup>1,3\*</sup>, Lynne E. Bilston<sup>1,4</sup>

<sup>1</sup> Neuroscience Research Australia, Margarete Ainsworth Building, Barker Street, Randwick NSW 2031, Australia.

<sup>2</sup> University of New South Wales, School of Medical Sciences, Wallace Wurth Building, Kensington, NSW 2052, Australia.

<sup>3</sup> Macquarie University, Department of Engineering, Faculty of Science, Macquarie University NSW 2109, Australia.

<sup>4</sup> University of New South Wales, Prince of Wales Clinical School, Edmund Blacket Building, Kensington, NSW 2052, Australia.

<sup>†</sup> These authors contributed equally to this work.

\*Corresponding author

E-mail: shaokoon.cheng@mq.edu.au

Word count: 3440

## Abstract

Information on pediatric brain tissue mechanical properties and, more pertinently, how they change during postnatal development remains scarce despite its importance to investigate mechanisms of neural injury. The aim of this study is to determine whether brain mechanical properties change in-vivo during early postnatal development in a rat model. Rat brain viscoelastic properties were measured longitudinally in ten healthy Sprague Dawley rats at five different time points from postnatal week one to week six using magnetic resonance elastography at 800Hz. Myelination and cell density were assessed histologically at the same time points to understand how the underlying tissue microstructure may be associated with changes in mechanical properties at different brain regions. Longitudinal changes in each variable were assessed using a generalized linear model with pairwise comparisons of means between weeks. The brain shear modulus in the cortical gray matter at postnatal week one was  $6.3 \pm 0.4$  kPa, and increased significantly from week one to week two (pairwise comparison,  $p < 0.01$ ), remained stable from week two to week four and decreased significantly by week six (pairwise comparison,  $p < 0.001$ ). In the deep gray matter, brain tissue stiffness at postnatal week one was  $6.1 \pm 2.0$  kPa, and increased significantly from one to week four (pairwise comparison,  $p < 0.05$ ) before decreasing significantly by week six (pairwise comparison,  $p < 0.001$ ). Stiffness changes were not directly correlated to histological observations. These data suggest that brain tissue shear modulus initially increases during a period equivalent to early childhood, and then decreases during a period equivalent to adolescence.

## Introduction

Research on brain tissue mechanical properties has grown exponentially over the last four decades (Cheng et al., 2008). Viscoelastic properties of the brain are important for understanding and predicting neural injury under a range of loading types and accurate mechanical properties are needed to improve the fidelity of computational brain models used to simulate complex mechanical loading related to these injuries (Chatelin et al., 2012; Cheng and Bilston, 2010). In addition, understanding changes in brain tissue mechanical properties in health and disease may provide new insights into pathological processes in the brain or form the basis for new biomarkers of disease.

The majority of previous measurements of brain tissue mechanical properties were obtained in-vitro but there is considerable variation in reported data, most likely due to differences in experimental conditions. For example, measurements obtained from in-vitro testing of brain tissues are likely to be affected by post-mortem time and pre-conditioning protocols (Cheng et al., 2009; Hrapko et al., 2008). Moreover, measurements may also be affected by the loss of perfusion and therefore may not represent the mechanical properties of living brain tissues reliably (Bilston, 2002). Nevertheless, in-vitro testing has provided useful insights into the mechanical response of the brain under shear (Bilston et al., 2001), compression (Rashid et al., 2012) and tension (Miller and Chinzei, 2002).

Magnetic resonance elastography (MRE) is a useful and rapidly developing technology that is able to measure the mechanical properties of soft biological tissues in-vivo and non-invasively in humans and animals (Green et al., 2008; Muthupillai et al., 1995; Schregel et al., 2012). This technique has been used to quantify how mechanical properties of living tissues are affected by disease processes such as cancer (Jamin et al., 2015; Pepin et al., 2015), liver fibrosis (Huwart et al., 2006) and sleep apnoea (Brown et al., 2015). In the brain, MRE studies have shown mechanical differences in the brains of patients with normal pressure hydrocephalus (Streitberger et al., 2011), and Alzheimer's disease, to name just a few.

Similar to other soft biological tissues, brain tissue mechanical properties change with age but data on the mechanical properties of pediatric brain tissue, particularly in the postnatal age group remains scarce. Although MRE has been used to show how brain tissue mechanical properties

change during aging in healthy adults (Sack et al., 2009), how these properties change during the early stages of brain development remain unclear. The primary aim of this study was to use MRE to characterize how shear moduli in the brain change during early postnatal development through to adolescence, using a rat model. We hypothesized that the shear moduli would change during development.

## Methods

### Animals

The study protocol was approved by the UNSW Animal Care and Ethics Committee (ACEC). Pregnant rats gave birth in the local animal house. Ten healthy Sprague Dawley rat pups (five female and five male) were randomly selected from two independent litters. Rat brain viscoelastic properties were measured at postnatal (PN) age one week old (PN6-9 days), two weeks old (PN12-16 days), three weeks old (PN19-22 days), four weeks old (PN26-31 days), and six weeks old (PN40-42 days), representing neonatal to juvenile animals. The neonatal rats were housed with their mothers until weaned at three weeks old. 3 - 4 weeks old animals were housed in a standard cage with normal 12 hour day/night lighting, and free access to water and food. All animals were checked daily and weighed prior to each scan.

### MR imaging

Anesthesia was induced with 2.5% inhaled isoflurane gas (mixed with 100% oxygen, flow rate 1L/min) and maintained during scanning at 0.5% - 1.5% for rats between one to three weeks old and 1.5% - 2% for rats between four to six weeks old. Body temperature was maintained at 36°C - 37°C with a water heating blanket, and respiration was monitored continuously. MR imaging was performed using a 9.4T MR scanner (Bruker BioSpec 94/20, Karlsruhe, Germany). Animals up to two weeks of age were scanned using a 50 mm diameter volume transmit/receive resonator coil. Animals from three to six weeks of age were scanned using an 86 mm diameter volume transmit resonator coil and a 20 mm diameter surface receive - only coil centered above the foramina of Monro.

T2 weighted anatomical axial images of the brain were obtained using a two dimensional rapid acquisition with relaxation enhancement sequence (TurboRARE), with the following parameters: repetition time /echo time = 3000 ms /9.5 ms, rapid acquisition with relaxation enhancement factor 16, twenty four signal averages, one repetition, nine contiguous slices, field of view = 19.2

mm × 19.2 mm, slice thickness = 300 μm, matrix = 128 × 128, acquisition time = 9 minutes 36 seconds. A multi slice multi echo MRE sequence (TE/TR= 28.75/2813.75ms) was used for the MRE acquisition (Schregel et al., 2012), in matching slice geometry. By consecutively applying motion-encoding gradients to three axes, the three dimensional propagation of the mechanical wave inside the brain was captured at eight time-points per vibration period. Acquisition time for each of the three directions was 24 minutes.

Mechanical vibrations (800 Hz) were induced in the rat brain using an acoustic shaker (Model 4890, Brüel & Kjær Sound & Vibration Measurement A/S Corp., Denmark) via a carbon fiber rod. Due to the increase in head size of the animals with age, the mechanical vibrations were introduced into the brain using two different mechanical transducer designs to optimize wave propagation. For animals up to three weeks old, vibration was transmitted via a flat rigid piston placed on top of the head. For older animals (four weeks and six weeks), vibration was transmitted via a bite bar attached to the teeth. Pilot studies were conducted to compare the two MRE setups on freshly sacrificed three week old rat carcasses (performed within 5 hours post-mortem at room temperature) and no significant differences in stiffness measurements were found between the two designs.

### Histology

In order to determine the myelination and cell density during brain development, rat brains were obtained from a different litter of rat pups with age similar to the rats used for imaging. Brain samples were fixed in 10% formaldehyde, embedded in paraffin, sectioned coronally, and counter stained in one batch with Luxol Fast Blue and Cresyl Violet.

### Data analysis and statistics

#### MRI Analysis

Cross-sectional area of the whole brain, deep gray matter and thickness of cortical gray matter were measured by manual segmentation using ImageJ (Version 1.45, NIH, Bethesda, MD; USA) and the regions of interest are shown in Figure 1. The cortical gray matter region was defined as the area between the corpus callosum and the pial surface. The cortical thickness was measured at five locations distributed equally across the cortical gray matter area. MRE reconstruction was performed using previously validated in-house software (Green et al., 2008), and shear modulus data for the cortical gray matter and deep gray matter were averaged over the three central imaging slices. The mechanical properties were quantified in terms of the magnitude of complex

shear modulus ( $G^*$ ). Datasets were considered reliable if the local total wave amplitude was greater than  $0.2\ \mu\text{m}$ . This value corresponded to approximately three times the total amplitude of the noise level (i.e.  $0.06\ \mu\text{m}$ ) based on pilot acquisitions where no mechanical wave was applied. Datasets with motion artifacts were also excluded from analysis. Based on the aforementioned criteria, approximately 13% of the MR elastography measurements were excluded.

Mean and standard deviation for each variable were calculated at each time point. Longitudinal changes in each variable were assessed using a generalized linear model with pairwise comparisons of means between weeks. All statistical analysis were performed using SPSS (v22, IBM, Armonk, New York, USA).

#### Semi-quantitative histology analysis for cell and myelin index

Coronal slices at the foramina of Monro were scanned using Scan Scope XT (Aperio; Vista, CA). Neuronal cells and myelination were estimated semi-quantitatively on nine selected 20X magnified regions (Figure 5A). The images were converted to 8-bit gray scale images (0-white, 255-black). To analyse cell density, image segmentation was first performed using the Otsu thresholding method and the number of neuronal cells was counted using a cell counter plugin. Cell density was then obtained by dividing the number of cells by the area of the selected region ( $2.52\ \text{mm}^2$ ). Myelin index was analyzed as described in Ihara et al (2010). Briefly, five different ranges of staining intensity (0-50, 51-100, 101-150, 151-200, and 201-250) were used to determine myelin index on the gray scale images. The median of each range was multiplied by the area (expressed as percentage of the selected region area) of the corresponding stained region for each range and these values were added to obtain the total myelin index.

## Results

Two rats died during the study and they were excluded from the analysis. Neither rat recovered from the anesthesia, and cause of death was likely related to suboptimal anaesthesia dosage and/or hypothermia. One rat died after the scan in week 4 and the other during the scan in week 6. For the rat that died in week 6, the anatomical scan was completed, but not the MR elastography.

#### Brain Growth

Figure 2 shows a set of T2 weighted anatomical images and MR elastograms from the same rat at different postnatal weeks. The average cross sectional area of the whole brain, cross sectional area

of the deep gray matter and thickness of the cortical gray matter are shown in figures 3B, 3C and 3D respectively. There was a rapid increase in brain size between week one and week two, followed by slower brain growth thereafter (see Figures 3B - 3D), even though the animals overall weight continued to increase (Figure 3A). Brain growth was reflected in a significant increase in the whole brain cross sectional area (pairwise comparison,  $p < 0.001$ ) and cortical gray matter thickness (pairwise comparison,  $p < 0.001$ ) from week one to week six. While the cortical gray matter thickness appeared to plateau after week three, there was a modest increase in whole brain cross sectional area and deep gray matter area in the same period. Both the cross sectional area of the whole brain and the deep gray matter increased by more than 50% between week one and week six (pairwise comparison,  $p < 0.001$  for both).

### Mechanical Properties

The measured shear moduli of the cortical gray matter and deep gray matter are presented in Figure 4. The brain shear modulus in the cortical gray matter and deep gray matter at postnatal week one were  $6.3 \pm 0.4$  kPa and  $6.1 \pm 2.0$  kPa respectively. There was spatial variation in the measured brain shear modulus, as can be seen in Figure 2, and considerable variability between younger animals in the deep gray matter. The shear modulus in the cortical gray matter increased from week one to week two, then remained stable from week two to week four before decreasing to be significantly lower in week six than at all other ages (see Figure 4A). In contrast, the shear modulus of the deep gray matter increased gradually between week one and week four (pairwise comparison,  $p < 0.05$ ) but was not significantly different between the intermediate time points (Figure 4B). Similar to what was observed in the cortical gray matter, the deep gray matter shear modulus was significantly lower at week six than at weeks three and four (pairwise comparison,  $p < 0.001$ ).

### Histology

Sample histology images are shown in Figure 5A, along with the analysis regions. Semi-quantitative analysis of the histological sections is shown in Figure 5B and 5C. Cell density in both the cortical gray matter and deep gray matter decreased from week one to week two, increased from week two to week four before decreasing in week six (Figure 5B). The Luxol fast blue staining (Figure 5C) indicated increasing myelination from week one to week six in both the cortical gray matter and deep gray matter, with the greatest increase being in the corpus callosum between week three and four.



## Discussion

This study is the first to quantify changes in brain shear modulus in vivo during early postnatal development, using a rat model. The age of the rats used in this study are approximately equivalent to the human ages of 2 to 12 years old (Quinn, 2005). The cortical gray matter stiffness increases from week one to week two and remains stable for three weeks before it decreases at week six. In the deep gray matter, tissue stiffness appears to increase gradually from week one to week four before it decreases at week six.

The increase in cortical gray matter stiffness from week one to week two occurs in parallel with rapid cortical growth that occurs during this period. This growth is thought to result primarily from an increase in average neuronal size and gliogenesis, rather than neurogenesis (Bandeira et al., 2009). Although a comprehensive characterization of changes in brain cellular composition with age cannot be assessed with only the histological stains used here, the same study (Bandeira et al., 2009) showed that there was a marked loss of neurons during the second and third postnatal week, which is accompanied by a further increase in glial cells. Therefore, the slower increase in brain tissue stiffness in the cortical gray matter between weeks 2 and 4 may be due to neuronal loss partially offsetting the effect of the increase in glial cells. Gliogenesis during postnatal development contributes substantially to the enlargement of brain structures (Hedin-Pereira et al., 1999) and this is demonstrated by the distinctive increase in cortical gray matter thickness and deep gray matter cross-sectional area from week 1 to week 3 in our study. It is also possible that vascular development could contribute to the changes in mechanical properties (Jugé et al., 2015). Histological studies of vascular development in the rat cortex suggest that vascular density is relatively sparse in the first 10 postnatal days (Caley and Maxwell, 1970), although there are many vascular sprouts forming in the latter half of that period (Rowan and Maxwell, 1981). In the following week, there is a rapid (approximately threefold) increase in vessel density in the cortex (Caley and Maxwell, 1970), in parallel with differentiation of simpler capillary-like blood vessels into arterial venous structures (Rowan and Maxwell, 1981). However, the time course of these changes does not closely follow the mechanical property changes, so the relationship between them is unclear.

While broadly similar trends in stiffness were observed in the deep gray matter and the cortex, the increase in stiffness was more gradual in the cortical gray matter over the first 4 weeks. The reasons for this are not fully clear, but the deep gray matter is punctuated by myelinated fiber bundles, and since myelin has a low shear modulus (Yamada and Evans, 1970), and white matter

has previously been shown to be slightly less stiff than gray matter (Green et al., 2008), more myelin in the deep gray matter may underlie the less apparent increase in tissue stiffness in the deep gray matter as compared to the cortical gray matter. However, a recent study has shown that Cuprizone-induced demyelination decreases brain parenchyma stiffness (Schregel et al., 2012), so the effects of myelin on tissue stiffness are not yet well-established. Although our histological evaluations showed increased myelination in the deep gray matter between week four to six, myelination intensity appeared to be similar to the cortical gray matter from week one to week three. A more detailed examination of the brain tissue microstructure may help to shed light on the slight difference between the changes in tissue stiffness between these two brain regions. Another plausible explanation for the less apparent increase in deep gray matter stiffness may be that there was more variability in the data due to the propagation of less than perfect mechanical waves into the deeper regions of the brain. In addition, changes in deep gray matter stiffness could also be affected by vascular development but as noted above, the time course of vascular development does not directly match the observed mechanical property changes, so any relationship between the two is not yet clear. Both the cortical and deep gray matter regions exhibited a significant reduction in shear modulus between weeks 4 and 6. At the same time, our histological evaluations showed an apparent decrease in cell density at week six in both these brain regions, but neuronal and glial cell numbers are thought to be reasonably stable at this time (Bandeira et al., 2009). This also coincides with a period (equivalent to adolescence in humans) during which there is substantial remodeling in the brain, including cell death and dendritic pruning (Brenhouse and Andersen, 2011) which could be responsible for the observed decrease in stiffness. Direct confirmation of the relationship of these processes on brain tissue stiffness requires more detailed histological analysis that was not possible in the current study, and thus this remains a working hypothesis.

A small number of other studies have examined brain mechanical properties during development. For example, Shulyakov et al (2011) performed indentation tests on live rat brains through an intact dura mater at different ages (between 10 to 180 days postnatal) and reported a significant increase in tissue stiffness with age. As the reported measurements are between 40 – 180 kPa, and were made through the dura, it is likely that these data are dominated by changes in the dura mater, with a lesser contribution from the underlying brain tissue since the dura mater is substantially stiffer than the brain. Thibault and Margulies (1998) showed that samples from frontal cerebrum in porcine neonates are stiffer than in adults when tested at small strains (more akin to the strains used in the current study) but less stiff when tested at large strains. The porcine

neonatal period is approximately equivalent to 2 weeks postnatal in rats, so these results are consistent with our data, which show the brain to be stiffer at this time than at the latest time point measured (6 weeks). In addition, differences in brain regions, experimental methods and conditions such as mechanical strain likely influence trends in brain stiffness observed with age, and may explain the discrepancies between existing studies. Perfusion pressure may also alter tissue stiffness, although the significance of this effect remains controversial (Bilston, 2002; Gefen and Margulies, 2004). For example, it is unclear how perfusion pressure changes during postnatal development but the rapid development of new blood vessels during this period does not appear to explain the observed tissue stiffness changes observed in our study.

There were several technical limitations in this study. First, reconstruction of the MR elastograms was based on the assumption that the brain is isotropic, despite the well-known structural anisotropy of white matter tracts, and the presence of some white matter bundles within the deep gray matter regions of interest at later time points. There have been recent approaches to reconstruct anisotropic properties from MRE, including our own work combining MRE with diffusion tensor imaging (DTI) (Qin et al., 2013). However, DTI data was not collected in the current study, due to the need to minimize scan times to avoid anaesthetic complications for the neonatal animals. Second, it was difficult to measure the shear modulus of smaller brain regions such as the corpus callosum in the neonatal rat due to spatial resolution limits. Although spatial resolution can be increased, this would require longer acquisition times which are undesirable for the well-being of anaesthetized animals.

In conclusion, this study has documented the changes in brain tissue stiffness in the cortical gray matter and deep gray matter in developing rats. Although the change in tissue stiffness during the first six weeks of postnatal development is slightly different in the two brain regions, brain tissue stiffness generally increases in the early postnatal period, equivalent to early childhood in humans, and decreased at postnatal week six, corresponding approximately to adolescence in humans. Histological examinations and other quantitative MR studies infer that these changes may be related to brain growth and remodeling processes and further studies are required to elucidate the detailed mechanisms of biomechanical properties changes in the brain during postnatal brain development.

## Conflict of interest statement

No conflicts of interest to declare.

## Acknowledgement

This research was supported by the Australian National Health and Medical Research Council (NHMRC). L.E.B. is supported by NHMRC research fellowship. There are no personal or financial conflicts to disclose by any of the authors of this manuscript.

## References

- Bandeira, F., Lent, R., Herculano-Houzel, S., 2009. Changing numbers of neuronal and non-neuronal cells underlie postnatal brain growth in the rat. *Proceedings of the National Academy of Sciences of the United States of America* 106, 14108–14113. doi:10.1073/pnas.0804650106
- Bilston, L.E., 2002. The effect of perfusion on soft tissue mechanical properties: a computational model. *Computer methods in biomechanics and biomedical engineering* 5, 283–90. doi:10.1080/10255840290032658
- Bilston, L.E., Liu, Z., Phan-Thien, N., 2001. Large strain behaviour of brain tissue in shear: some experimental data and differential constitutive model. *Biorheology* 38, 335–45.
- Brenhouse, H.C., Andersen, S.L., 2011. Developmental trajectories during adolescence in males and females: a cross-species understanding of underlying brain changes. *Neuroscience and biobehavioral reviews* 35, 1687–703. doi:10.1016/j.neubiorev.2011.04.013
- Brown, E.C., Cheng, S., McKenzie, D.K., Butler, J.E., Gandevia, S.C., Dsc, M., Bilston, L.E., 2015. Tongue Stiffness is Lower in Patients with Obstructive Sleep Apnea during Wakefulness Compared with Matched Control Subjects. *Sleep* 38, 537.
- Caley, D.W., Maxwell, D.S., 1970. Development of the blood vessels and extracellular spaces during postnatal maturation of rat cerebral cortex. *The Journal of Comparative Neurology* 138, 31–47. doi:10.1002/cne.901380104
- Cheng, S., Clarke, E.C., Bilston, L.E., 2009. The effects of preconditioning strain on measured tissue properties. *Journal of Biomechanics* 42, 1360–1362. doi:10.1016/j.jbiomech.2009.03.023
- Cheng, S., Clarke, E.C., Bilston, L.E., 2008. Rheological properties of the tissues of the central nervous system: A review. *Medical Engineering and Physics* 30, 1318–1337. doi:10.1016/j.medengphy.2008.06.003
- Gefen, A., Margulies, S.S., 2004. Are in vivo and in situ brain tissues mechanically similar? *Journal of Biomechanics* 37, 1339–1352. doi:10.1016/j.jbiomech.2003.12.032
- Green, M.A., Bilston, L.E., Sinkus, R., 2008. In vivo brain viscoelastic properties measured by magnetic resonance elastography. *NMR Biomed* 21, 755–764. doi:10.1002/nbm.1254
- Hedin-Pereira, C., Lent, R., Jhaveri, S., 1999. Morphogenesis of callosal arbors in the parietal cortex of hamsters. *Cerebral cortex (New York, N.Y. : 1991)* 9, 50–64.

- Hrapko, M., van Dommelen, J. a W., Peters, G.W.M., Wismans, J.S.H.M., 2008. The influence of test conditions on characterization of the mechanical properties of brain tissue. Journal of biomechanical engineering 130, 031003. doi:10.1115/1.2907746
- Huwart, L., Peeters, F., Sinkus, R., Annet, L., Salameh, N., ter Beek, L.C., Horsmans, Y., Van Beers, B.E., Beek, L.C., Horsmans, Y., Beers, B.E. Van, ter Beek, L.C., Van Beers, B.E., 2006. Liver fibrosis: non-invasive assessment with MR elastography. NMR Biomed 19, 173–179. doi:10.1002/nbm.1030
- Jamin, Y., Boulton, J.K.R., Li, J., Popov, S., Garteiser, P., Ulloa, J.L., Cummings, C., Box, G., Eccles, S.A., Jones, C., 2015. Exploring the Biomechanical Properties of Brain Malignancies and their Pathological Determinants In Vivo with Magnetic Resonance Elastography. Cancer Res canres. 1997.2014. doi:10.1158/0008-5472.CAN-14-1997
- Jugé, L., Petiet, A., Lambert, S.A., Nicole, P., Chatelin, S., Vilgrain, V., Van Beers, B.E., Bilston, L.E., Sinkus, R., 2015. Microvasculature alters the dispersion properties of shear waves – a multi-frequency MR elastography study. NMR in Biomedicine 28, 1763–1771. doi:10.1002/nbm.3438
- Miller, K., Chinzei, K., 2002. Mechanical properties of brain tissue in tension. Journal of Biomechanics 35, 483–490. doi:10.1016/S0021-9290(01)00234-2
- Muthupillai, R., Lomas, D.J., Rossman, P.J., Greenleaf, J.F., Manduca, a, Ehman, R.L., 1995. Magnetic resonance elastography by direct visualization of propagating acoustic strain waves. Science (New York, N.Y.) 269, 1854–1857. doi:10.1126/science.7569924
- Pepin, K.M., Ehman, R.L., McGee, K.P., 2015. Magnetic Resonance Elastography (MRE) in Cancer: Technique, Analysis, and Applications. Progress in Nuclear Magnetic Resonance Spectroscopy. doi:10.1016/j.pnmrs.2015.06.001
- Qin, E.C., Sinkus, R., Geng, G., Cheng, S., Green, M., Rae, C.D., Bilston, L.E., 2013. Combining MR elastography and diffusion tensor imaging for the assessment of anisotropic mechanical properties: a phantom study. Journal of magnetic resonance imaging : JMRI 37, 217–26. doi:10.1002/jmri.23797
- Rashid, B., Destrade, M., Gilchrist, M.D., 2012. Mechanical characterization of brain tissue in compression at dynamic strain rates. Journal of the Mechanical Behavior of Biomedical Materials 10, 23–38. doi:10.1016/j.jmbbm.2012.01.022
- Rowan, R. a, Maxwell, D.S., 1981. Patterns of vascular sprouting in the postnatal development of the cerebral cortex of the rat. The American journal of anatomy 160, 247–55. doi:10.1002/aja.1001600303
- Sack, I., Beierbach, B., Wuerfel, J., Klatt, D., Hamhaber, U., Papazoglou, S., Martus, P., Braun, J., 2009. The impact of aging and gender on brain viscoelasticity. NeuroImage 46, 652–7. doi:10.1016/j.neuroimage.2009.02.040
- Schregel, K., Wuerfel, E., Garteiser, P., Gemeinhardt, I., Prozorovski, T., 2012. Demyelination reduces brain parenchymal stiffness quantified in vivo by magnetic resonance elastography. Proceedings of the National Academy of Sciences of the United States of America 109, 6650–6655. doi:10.1073/pnas.1200151109/- /DCSupplemental.www.pnas.org/cgi/doi/10.1073/pnas.1200151109
- Streitberger, K.-J., Wiener, E., Hoffmann, J., Freimann, F.B., Klatt, D., Braun, J., Lin, K., McLaughlin, J., Sprung, C., Klingebiel, R., Sack, I., 2011. In vivo viscoelastic properties of the brain in normal pressure hydrocephalus. NMR in biomedicine 24, 385–92.

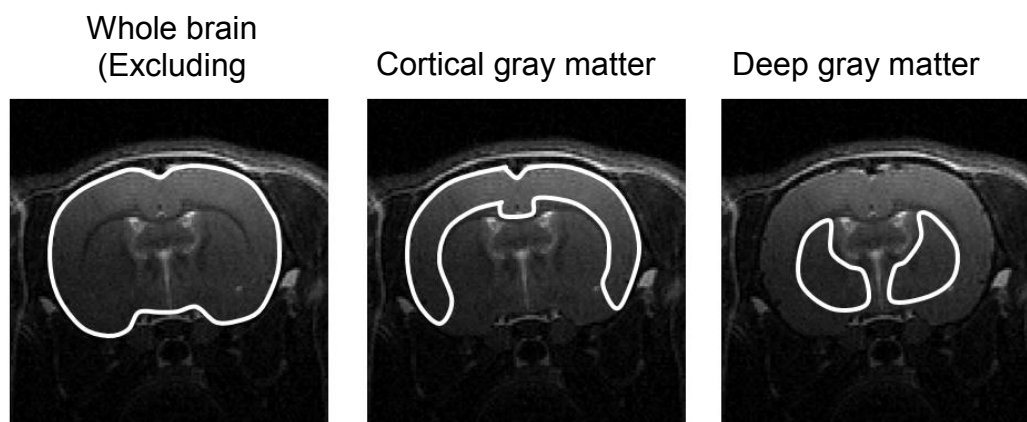


**Figure 1.** Representative anatomical images of a 6 weeks old rat brain showing regions of interest - whole brain, cortical gray matter and deep gray matter.

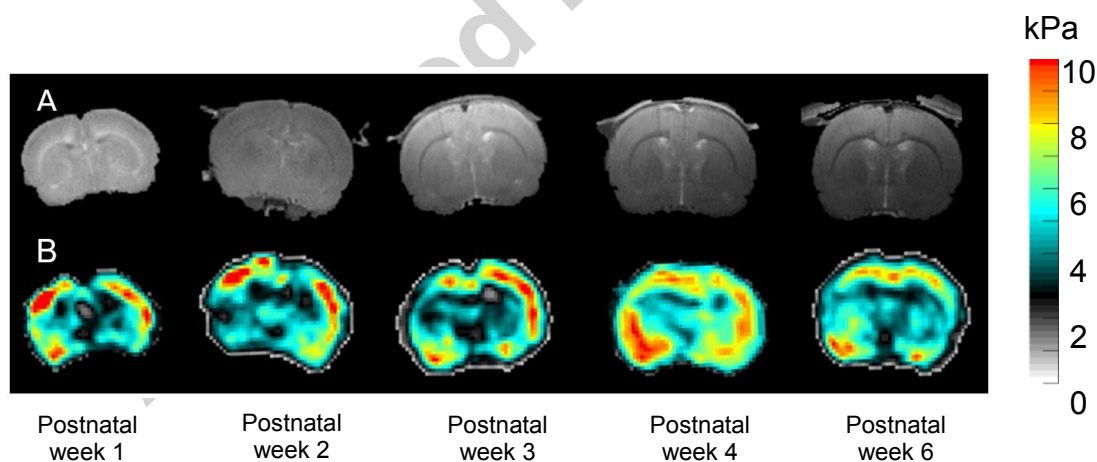


**Figure 2.** (A) Representative T2-weighted coronal MRI images at the level of foramina of Monro, and (B) MR elastograms of a typical animal from week one to six with the shear modulus in kPa. NB: Tissue around the brain was cropped in the T2-weighted images.

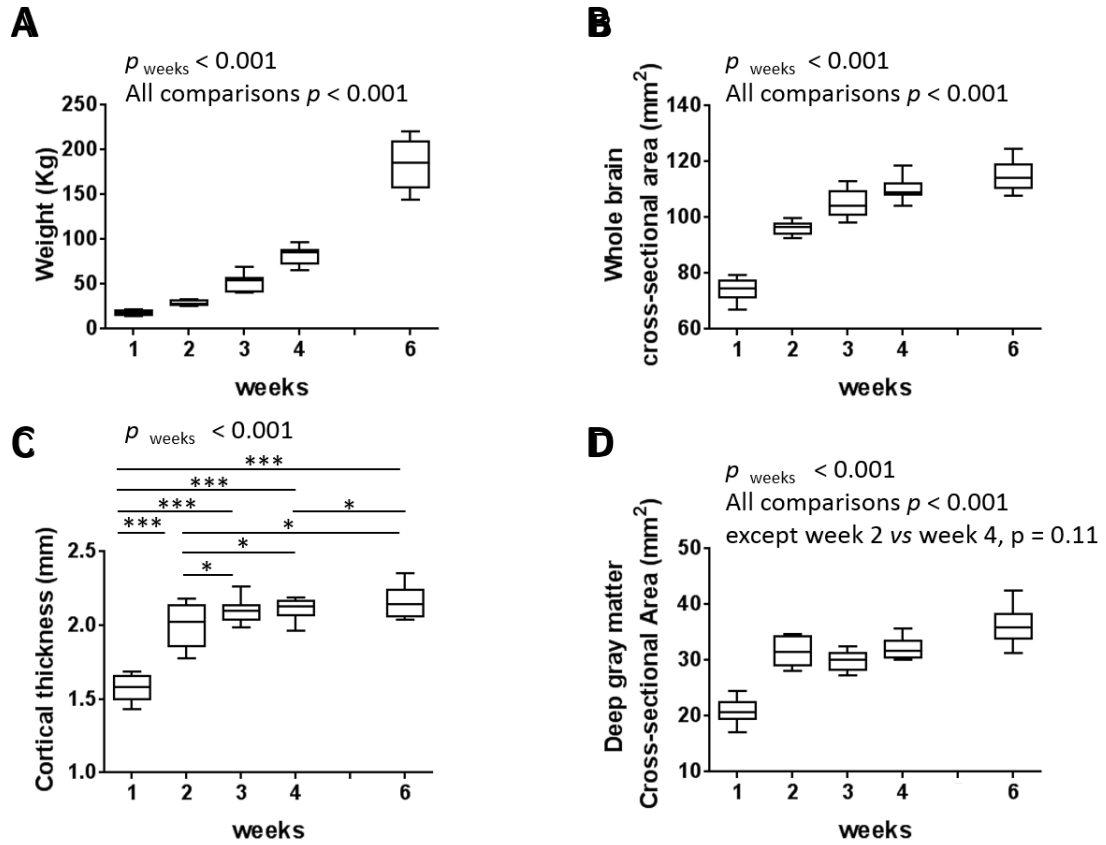


**Figure 3.** Panels show whisker & box plots of (A) body weight of rats, (B) whole brain cross-sectional area, (C) cortical gray matter thickness and (D) deep gray matter cross-sectional area against age in weeks. Longitudinal changes in each variables were assessed using a generalized linear model (see  $p_{\text{weeks}}$ ) with pairwise comparisons of means between weeks. Asterisks denote significant comparisons - \*:  $0.01 < p < 0.05$ , \*\*:  $0.001 < p < 0.01$ , \*\*\*:  $p < 0.001$ .

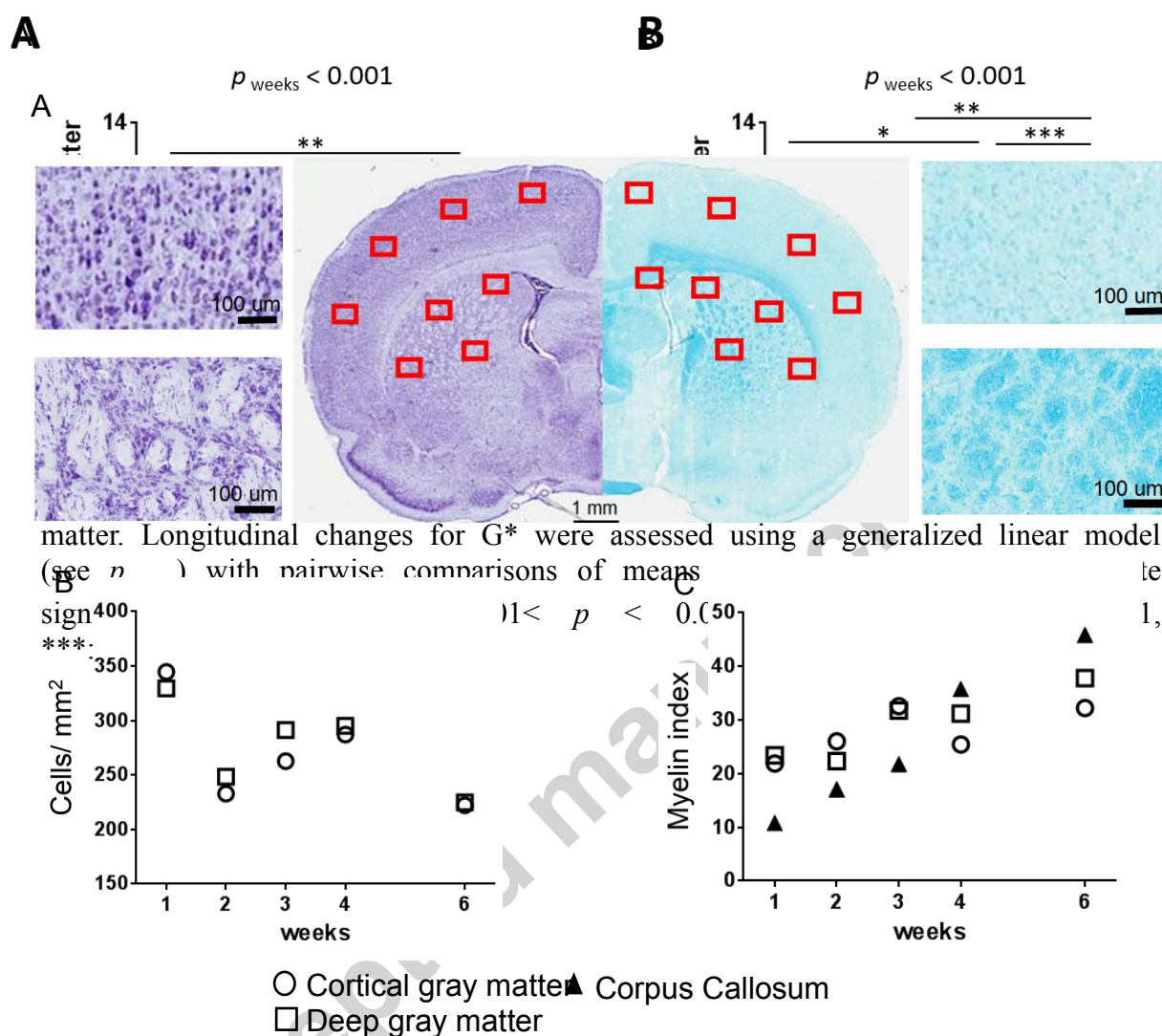


**Figure 5.** (A) Representative histology slices at the foramina of Monro of a six week old rat. Left panels show Cresyl violet staining and right panels show Luxol Fast Blue staining. (B) Semi-quantitative results for cell density assessed by the mean number of cells per mm<sup>2</sup> and (C) extent of myelination represented by the relative Luxol Fast Blue area with the age of the animal (in weeks postnatal). Cell density and myelination estimates were based on 8 cortical gray matter, 8 deep gray matter and one corpus callosum regions indicated by the red colored boxes (not drawn to scale) in Figure 5A.